

# Simulation and 3-D Visualization of Crystallization Process Based on Cellular Automata

Jiali Ai\*. Jindong Dai\*. Chi Zhai\*\*<sup>1</sup>. Wei Sun.\*<sup>1</sup>

\* College of Chemical Engineering, Beijing University of Chemical Technology, Beijing, 100029 China (Tel: 010-64445826; e-mail: sunwei@mail.buct.edu.cn).

\*\* Faculty of chemical engineering, Kunming University of Science and Technology, Kunming, 650500 China (e-mail: zhaichi@kmust.edu.cn)

---

**Abstract:** Crystallization is widely used for separation and purification. During this process, the different growth conditions, such as temperature and supersaturation, would result in different size and morphology, which not only affect the product quality, but also affect the subsequent process operations. Through the simulation of the crystallization process, a better understanding of crystallization process dynamics can be extracted. The population balance (PB) model has been used to simulate industrial crystallization processes, while the multi-dimensional population balance (MPB) model can be used to obtain the information of size and morphology distribution. However, the morphological distribution information provided by numerical solution of MPB is macroscopic, and the specific morphology of a crystal particle cannot be displayed at the microscopic level, so the difference among crystals morphology cannot be clearly displayed. Cellular automata (CA) is a method that simulates a process by considering simple cell changes and cell-to-cell interactions. It can be employed to conduct cross-scale simulation, i.e., both macro and micro. In this work, a CA method is introduced into an MPB model to simulate the batch cooling crystallization process from solution. The rule of crystal growth comes from classical diffusion theory, and whether the solution is transformed into a crystal is realized by the Monte Carlo method. The crystallization of potassium dihydrogen phosphate (KDP) is taken as a case-study and the results is verified with the results in the literature. Through CA simulation, not only the macroscopic crystal size and morphology distribution information can be obtained, but also the crystal morphology in microscopic can be exhibited. At the same time, the crystallization process can be visualized in 3-D environment, with size and morphology distribution being presented intuitively. In addition, the calculation time is reduced under certain accurate conditions. This result provides a theoretical reference for modeling, analysis and controlling of the crystallization process in the future.

**Keywords:** multi-dimensional population balance (MPB) equation, batch cooling crystallization of solution, dynamic simulation, potassium dihydrogen phosphate (KDP), High-resolution finite volume method, crystal morphology, crystal size distribution.

---

## 1. INTRODUCTION

Crystallization is a widely used unit operation and has been applied in various industrial fields. As granular products obtained by crystallization process, morphology and size are key parameters closely related to physical properties such as stability, solubility and fluidity (Tiwary and Jindal, 2012). They are not only influenced by the microstructure of crystals, but also by different growth environments, such as temperature and supersaturation (Misra et al., 2020). Therefore, it is necessary to study how to select appropriate crystallization conditions to produce crystal products with specific morphology, and simulation is a good research method, by which, various production conditions in the crystallization process can be systematically analyzed, so as to guide experimental research and production process, and effectively improve the production efficiency and product quality.

Generally, the simulation of the crystallization process is to establish a mathematical model based on population balance (PB) equation, and then to solve it by a discrete method such as finite volume (Gunawan et al., 2004). For example, Joseph et al. (2014) studied the size and morphology of the crystals during continuous crystallization of protein according to the PB. Rosa and Braatz (2018) used PB and the open-source CFD package OpenFOAM to study the methanol-water antisolvent crystallization process of lovastatin in a continuous flow tubular crystallizer with radially mixing. This method enables people to have a macroscopic understanding of the crystallization. On one hand, the nonlinearity of these mathematical models makes it difficult to solve. On the other hand, only the size and morphology distribution of crystals can be obtained by this method. It is difficult to understand the crystal morphology as intuitively as the scanning electron microscope image of the experimental results. Therefore, if

---

<sup>1</sup> corresponding author

there is a simulation method that can not only show the distribution of crystal size and morphology on the macro level, but also show the morphology of micro crystal with relatively simple calculation, the crystallization process can be better understood and visualized.

Cellular automata (CA) is a parallel computing method proposed by Von Neumann and Stanislaw Ulam in 1948. It describes physical and chemical processes by simple changes of subsystems and their interactions without solving partial differential equations and decoupling complex systems. Meanwhile, the discrete description of CA is convenient for computer visualization. Therefore, the CA can be used as a simulation method for crystallization process, which can realize relatively simple calculations and exhibit the microstructure and macro distribution of crystals at the same time. Many scholars have used CA to simulate the crystallization process (Liu et al., 2020). For example, Pineau et al. (2020) used CA to simulate silicon crystallization. In their work, the evolution rule is the most important part of CA, which is based on the oriented attachment rule. It is very suitable for melting crystallization or recrystallization processes. However, for the solution crystallization process, bulk transformation and surface reaction are the dominant factors of the crystallization process, because the distance between each crystal is too far and the system is away from the equilibrium state. The aging rule of oriented attachment at equilibrium state is not suitable for solution crystallization.

In this work, a method for simulating solution crystallization process by CA is proposed. The paper is organized as follows: the second part introduces how to use CA to simulate the batch cooling crystallization process. Then, in the third part, this method is demonstrated by taking potassium dihydrogen phosphate (KDP) as a case study. The simulation results of the size distribution are compared with those in the literature, and detailed in the fourth part. The last is a summary of the full text.

## 2. CA MODEL OF BATCH COOLING CRYSTALLIZATION OF SOLUTION

In order to simulate the batch crystallization process of solution cooling by the CA model, it is assumed:

- There is no crystal aggregation and breakage in the crystallization process, and only the nucleation and growth of crystals are considered in this CA model.
- The dissolution of crystals is not considered during the crystallization process.

Although these assumptions make the model not completely consistent with the actual solution cooling crystallization process, the main crystallization mechanisms can be well captured for crystallization nucleation and growth in certain solution crystallization process, as aggregation, breakage and dissolution have little effect on the crystallization process. Under these assumptions, the PB equation of batch cooling crystallization is shown in (1).

$$\frac{\partial f(L_i, t)}{\partial t} + \frac{\partial [G_i(L_i, t)f(L_i, t)]}{\partial L_i} = B(t)\delta(L_i) \quad (1)$$

where  $L_i$  represents the characteristic crystal length of dimension  $i$ ,  $f(L_i, t)$  represents the size distribution of the crystal at time  $t$ ,  $G_i(L_i, t)$  represents the growth rate of the length of  $L_i$  in the  $i$ -dimensional growth direction of the crystal at time  $t$ ,  $B(t)$  represents the nucleation rate at time  $t$ ,  $\delta(L_i)$  is the Dirac function, and the value at 0 point is 1, and the value at other places is 0.

### 2.1 Choice of CA Grid

The grid type is the first part to be determined in CA simulation. For the convenience of simulation, a two-dimensional square grid is selected to simulate crystallization (Fig. 1). Although the real crystal process should be more complex than this grid, its realization is relatively simple and reasonable for the mesoscopic growth model.

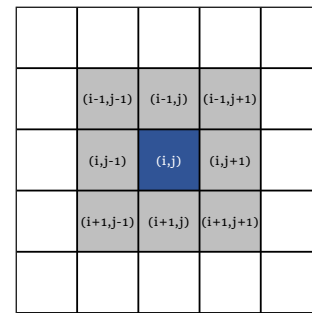


Fig. 1. Schematic diagram of CA grid and Moor type neighbours. The blue represents the central cell and the grey represents the neighbours.

### 2.2 For a cell: Subsystem evolution rules

In order to simulate the solution crystallization process, each cell consists of three parameters, namely the crystalline state ' $U$ ', the concentration state ' $C$ ', and the length state ' $L_i$ '. The crystalline state parameter ' $U$ ' takes two values, 0 and 1, corresponding to the solution and the crystal respectively. According to the hypothesis, there is no crystal dissolution in the model, and only when certain conditions are met, the cell state will change from solution state to crystal state. For the initial state, most of the cells are in the solution state and some cells are in the crystal state. These crystal state cells are chosen to represent the seed crystals added to the solution. After that, a probability  $P$  is obtained according to the nucleation rate to determine whether ' $U$ ' changes from 0 to 1. The initial concentration state of the model is same and equal to the initial concentration, which represents a state of uniform mixing. Then the change of the cell concentration state is determined by two parts, i.e., a. the solute reduction caused by crystallization forms a concentration gradient, b. diffusion caused by concentration gradient according to Fick's Law. As each cell contains the characteristic length parameter ' $L_i$ ', the length of each cell doesn't need to be specified for the simulation of such a grid. It is worth noting that in order to enable the crystal length to be calculated by this method, the  $L_i$  here is discretized compared to (1). Because there is no

aggregation and breakage of crystals in the model, the change of characteristic length is only based on the growth of crystals.

### 2.3 Neighbors

As can be seen from the previous section, in this model, each cell is described by three state parameters. Because there is no aggregation and breakage of crystals in the model, neither the crystal parameters nor the characteristic length parameters are affected by other cells. Only the concentration parameter needs to be decided by the concentration of neighbor cells. Since concentration diffusion is usually isotropic in space, a very common definition of cell neighborhood is the molar type, as shown in Fig. 1.

### 2.4 Dynamic Rules in CA

The evolution rule of CA needs to conform to the growth rule of crystal. The most commonly used theory to explain the crystallization process is the classic crystallization diffusion theory. It describes the growth of crystals in solution through the following three steps:

- solute moves around the crystal through random molecular motion;
- solute molecules react on the crystal surface and are embedded in the crystal lattice;
- in the previous step, the heat generated by the solute molecules embedded into the crystal lattice was transferred to the solution.

In this model, the evolutionary law of CA can be divided into two parts according to the classical diffusion theory of crystal growth: the internal change law of cells and the external change law affected by neighbors. Here, according to (a), the concentration parameter is not only affected by the internal change law of the cell based on the principle of conservation of mass, but also by Fick's law. According to (b), the crystal state parameter and the characteristic length parameters of the cell are only affected by the internal changes of the cell. The exotherm during the crystallization process is ignored.

## 3. A CASE STUDY: KDP BATCH COOLING CRYSTALLIZATION

In this section, a batch KDP crystallization process is chosen as a case study, the detailed parameters of KDP are taken from Gunawan et al. (2004) and presented as follows.

### 3.1 Parameters of batch crystallization system for KDP

The crystal morphology of KDP is shown in the Fig. 2. There are two characteristic lengths  $L_1$  and  $L_2$  for it. The volume of a single crystal can be calculated by (2)

$$V_0 = \frac{1}{3}L_1^3 + (L_2 - L_1) \cdot L_1^2 \quad (2)$$

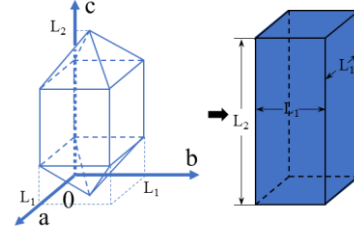


Fig. 2. Crystal diagram of KDP.

The growth rate and nucleation rate (in (1)) of the  $i$ -th dimension according to Gunawan et al. (2004) will be determined by (3) and (4), respectively.

$$G_i(L_i, t) = 0.1k_{gi}\left(\frac{c}{c_{sat}(T)} - 1\right)^{g_i}(1 + 0.6L_i), \quad i = 1, 2 \quad (3)$$

$$B(t) = k_b V \left(\frac{c}{c_{sat}(T)} - 1\right)^b \quad (4)$$

where  $c$  represents the concentration of the solution,  $c_{sat}(T)$  represents the saturation concentration at temperature  $T$ , using the data of (5).

$$\begin{aligned} c_{sat}(T) &= 9.3027 \times 10^{-5}T^2 - 9.7629 \times 10^{-5}T \\ &+ 0.2087 \quad g/g \text{ water} \end{aligned} \quad (5)$$

The relationship between temperature and time  $t$  is shown in (6).

$$T(t) = 32 - 4(1 - e^{-t/310}) \quad (6)$$

The values of all parameters are shown in Table 1 (Gunawan et al., 2004).

**Table 1. Parameters related to crystallization process of KDP (Gunawan et al., 2004)**

parameter	value	unit
$b$	2.04	-
$k_b$	$7.49 \times 10^{-8}$	number/ $\mu\text{m}^3$ /s
$g_1$	1.48	-
$g_2$	1.74	-
$k_{g1}$	12.1	$\mu\text{m}$ /s
$k_{g2}$	100.75	$\mu\text{m}$ /s
$\rho_c$	$2.11 \times 10^{-12}$	g/ $\mu\text{m}^3$

### 3.2 CA state variables and initialization

For the grid space of CA, the more grids, the more crystals that can be simulated, which means the higher precision, but also means the higher demand for computer resources. After compromise, a grid of  $A^2 = 1000 \times 1000$  was selected as the CA grid with the range of  $n^2 = 150\mu\text{m} \times 150\mu\text{m}$ , and the initial crystals size distribution is determined by (7).

$$f_0 = \begin{cases} -3.48 \times 10^{-4}(L_1^2 + L_2^2) & 18.05\mu\text{m} \leq L_1, L_2 \\ +0.136(L_1 + L_2) - 26.6 & L_1, L_2 \leq 21.05\mu\text{m} \\ 0 & \text{others} \end{cases} \quad (7)$$

For this CA model, the number of crystal particles can not be directly expressed in the form of crystals size distribution. Monte Carlo method is employed to set a probability  $P_0$ , so that the state of some cells can be changed from solution state to crystal state, i.e.  $P_0$  of cells it is  $U = 1$  and others  $U = 0$ . Here  $P_0$  is determined by (8). The crystalline state of  $100 \times P_0\%$  of the cells is  $U = 1$  and the crystalline state of  $(1 - 100 \times P_0\%)$  of the cells is  $U = 0$ .

$$P_0 = \int_0^\infty f_0 dL \cdot n^2 / A^2 \quad (8)$$

In this CA model, each cell represents a crystal or solution. There are three parameters: length, width and height, for better display of each crystal. According to Fig. 2, the KDP is in the shape of a cube biconical cone. Here, it is assumed that each KDP crystal is a cuboid with a side length  $L_1$  at the bottom and a height  $L_2$ . The initial state of the CA simulation is illustrated in Fig.3 and Fig.4.

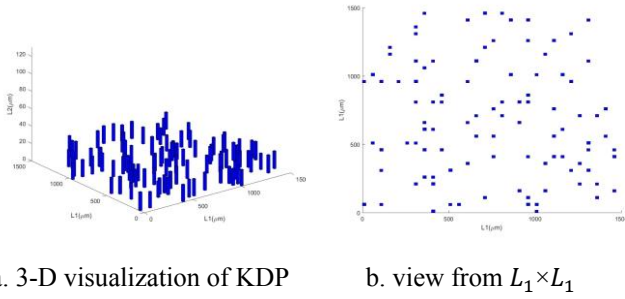


Fig. 3. Simulation result of the crystal morphology at the initial state by CA.

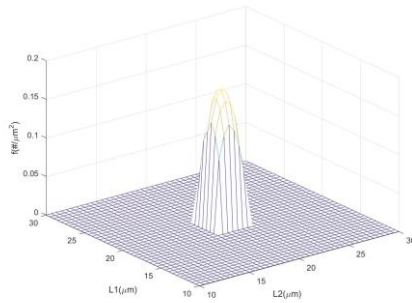


Fig. 4. Simulation result of the particle size distribution at the initial state by CA.

If the crystals of each cell are counted according to different sizes, the particle size distribution of the simulated can be obtained. In order to better compare with the simulation results in the literature, each scale is separated by  $0.5\mu\text{m}$ , and the number of crystals is per square micrometer (Fig. 4).

For the cell in crystal state, its characteristic length parameters are updated as shown in (9).

$$L_i^{t+1}(i, j) = L_i^t(i, j) + \Delta t G_i(i, j) \quad (9)$$

No mixing is considered in this model, so the concentration state of cells is only affected by its own crystallization and Fick's Law (if there is mixing, the bulk flow needs to be added to the rules of interaction among cells). According to the mass conservation equation, the concentration of the solution changes with time shown in (10), where  $\rho_c$  is the crystal density. Here, it is assumed that the size of the newly formed crystal and the consumption of solute can be neglected.

$$\frac{dc}{dt} = -\rho_c \int_0^\infty \int_0^\infty (2G_1(L_1 L_2 - L_1^2) + G_2 L_1^2) f dL_1 dL_2 \quad (10)$$

In this model, the change rule of cell concentration parameters can group into two types according to the crystal state parameters. For cells in the solution state ( $U=0$ ), the update of the cell concentration state is only based on the diffusion. For cells in the crystal state ( $U=1$ ), the update of the cell concentration state is not only based on diffusion, but also on the influence of solute consumed by crystal growth on the concentration state. Usually the diffusion rate of the concentration should be calculated according to Fick's law. But here, for simplicity of calculation, it is expressed as an average value, as shown in (11). It is the law of the change of the cell concentration state when  $U=0$ , and (12) is the law of the change of the cell concentration state when  $U=1$ . Compared with (11), (12) is based on (11) minus the concentration reduction caused by crystallization

$$C^{t+1}(i, j) = \frac{3}{8} C^t(i, j) + \frac{1}{8} \sum_{n=-1}^1 \sum_{m=-1}^1 (C^t(i+n, j+m)) \quad (11)$$

$$C^{t+1}(i, j) = \frac{3}{8} (C^t(i, j) - \rho_c (2G_1(i, j)(L_1(i, j)L_2(i, j) - L_1(i, j)^2) + G_2(i, j)L_1(i, j)^2) \Delta t) + \frac{1}{8} \sum_{n=-1}^1 \sum_{m=-1}^1 (C^t(i+n, j+m) - \rho_c (2G_1(i+n, j+m)(L_1(i+n, j+m)L_2(i+n, j+m) - L_1(i+n, j+m)^2) + G_2(i+n, j+m)L_1(i+n, j+m)^2) \Delta t) \quad (12)$$

At the same time, due to the nucleation of crystals, cells in solution state are partially transformed into crystal state. This transition probability  $P$  is defined by (13) according to (1) and (4).

$$P = BG / (A^2 - \sum U) \quad (13)$$

The time interval  $\Delta t = 0.01\text{s}$ .

#### 4. SIMULATION RESULT AND COMPARISON WITH HIGH-RESOLUTION FINITE VOLUME METHOD

In the above two sections, how to use this CA method to simulate the crystallization process of KDP batch cooling solution is introduced in detail. In this section, the simulation results are displayed. In order to valid the proposed method, the simulation results of crystal size distribution are compared with the high-resolution finite volume method which is proved feasible in the literature.

#### 4.1 3D visualization of CA simulation results

This model is used to simulate the crystallization process of KDP batch cooling solution for 100 seconds, and the simulation results are shown in the Fig. 5. and Fig. 6.

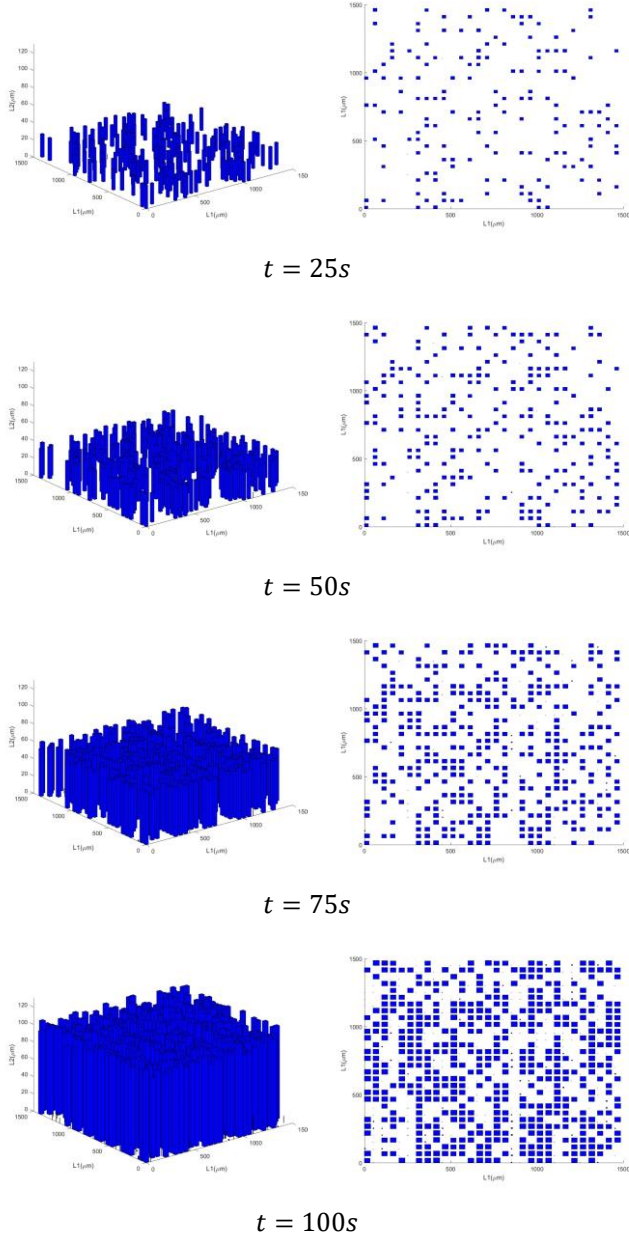


Fig. 5. Simulation result of the crystal morphology at 100s state by CA.

The Fig. 5 shows part of crystal morphology simulated by CA method. It can be clearly seen that with the extension of simulation time, KDP crystals gradually change from short and thick to slender. Similarly, in order to compare with the results of the literature, Fig. 6 shows the crystals size distribution per square micrometer with an interval of  $0.5\mu m$  simulated by the CA method.

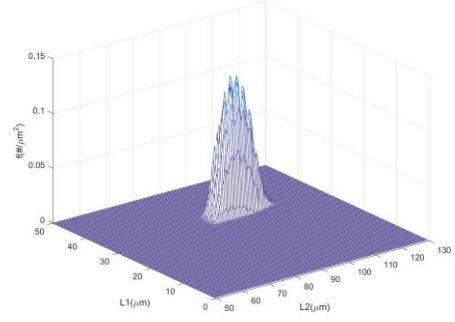


Fig. 6. Simulation result of the crystal morphology at 100s state by CA.

#### 4.2 High-resolution finite volume method and its result

As a numerical simulation method, the high-resolution finite volume method has been applied to the crystallization system to obtain discrete particle size distribution. Compared with other numerical simulation methods to obtain the particle size distribution, this method is a reliable simulation method, with higher accuracy in simulating the crystallization process. The detail of High-resolution finite volume method is shown in (14).

$$f_L^{t+1} = f_L^t - \frac{\Delta t}{\Delta d} (G_L f_L^t - G_{L-1} f_{L-1}^t) - \frac{k G_L}{2 \Delta d} (1 - \frac{k G_L}{\Delta d} (f_{L+1}^t - f_L^t) \phi_L + \frac{k G_{L-1}}{2 \Delta d} (1 - \frac{k G_{L-1}}{\Delta d} (f_L^t - f_{L-1}^t) \phi_{L-1}) \quad (14)$$

The same initial state as CA method is selected as the initial state of high-resolution finite volume method. The particle size distribution of the initial state simulated by the high-resolution finite volume method is shown in Fig. 7.

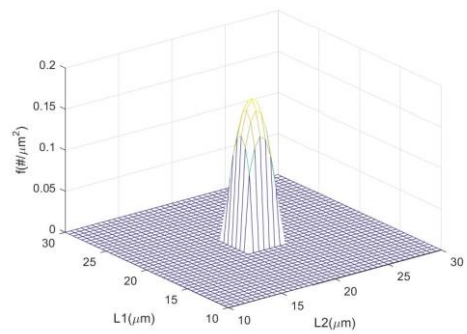


Fig. 7. Simulation result of the particle size distribution at the initial state by high-resolution finite volume method.

In order to compare the simulation results of the two methods better, model parameters are not changed, such as the time interval is still  $\Delta t = 0.01s$  and the space interval is  $\Delta d = 0.5\mu m$ . The flow limit function  $\phi_L$  adopts Van Leer flux limiter (Van Leer, 1974). After 100 seconds of operation, the crystal size distribution is shown in Fig. 8.

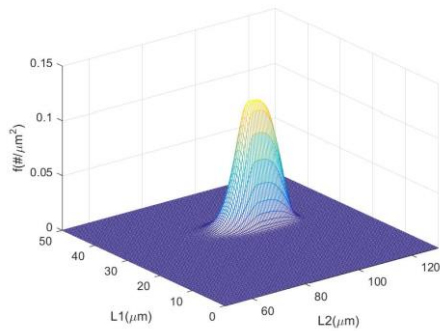


Fig. 8. Simulation result of the particle size distribution at 100s by high-resolution finite volume method.

#### 4.3 Comparison of the two methods

It can be seen that the results of crystal size distribution simulated by CA (Fig. 4 and Fig. 6) are similar to those simulated by the high-resolution finite volume method (Fig. 7 and Fig. 8). At the same time, the total volume of crystals within 1 square micron simulated by the two methods is counted, and the comparison shows that the changing trend of the two methods is the same (Fig. 9). These results prove that it is feasible to study the crystallization process by using this CA method.

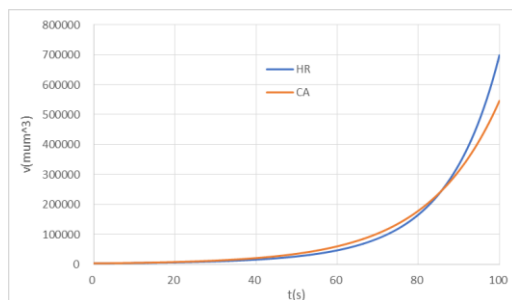


Fig. 9. The comparison of the total volume of the crystal of the cell automata and the high-resolution finite volume method.

It can be noted that CA can not only display the size distribution of crystals obtained by ordinary numerical simulation, but also 3-D visually display the morphological changes of each crystal (Fig. 4 and Fig. 6). According to the Fig. 6, the KDP crystal morphology changes from the short and thick of the seed to more slender. The results show that under this production condition, the longer the crystallization process, the finer the crystal morphology. If slender crystals are needed, this state can be maintained, and the crystallization process should continue. If this slender crystal morphology is not expected, production conditions needs to adjust. This kind of information can't be visually displayed by ordinary numerical simulation, but it can be displayed by this method.

## 5. CONCLUSIONS

In this paper, a novel CA method is used to simulate the crystallization process of KDP solution batch cooling, and compared with the simulation results of literature high-

resolution finite volume method. It is proved that CA is feasible to simulate the batch cooling solution crystallization process. Compared with the traditional method, this method can visually display the results of the microscopic crystal state, which is similar to the results of the scanning electron microscopy after the crystal growth experiment. At the same time, equivalent to the ordinary numerical simulation method, the size distribution of crystals can also be obtained by using this method. Compared with the high-resolution finite volume method in literature, its accuracy level is similar when computing environment, research objects and conditions are set the same.

Due to the limitation of this work, the influence of mixing on the crystallization process was not considered. In fact, this method is easier to add the influence of mixing and other factors on the process than the traditional method, because it only needs to change the law of interaction among cells and does not need to solve the Navier-Stoke equation. For other systems, the same methods can be used to study the crystallization process of solution. This method provides a new research method for the study of crystallization process, and also provides a better reference for the control of crystallization process.

**Acknowledgements:** The National Natural Science Foundation of China (Grant No. 21878012).

## REFERENCES

- Gunawan R., Fusman I., and Braatz R.D. (2004). High resolution algorithms for multidimensional population balance equations. *AIChE. J.*, 50(11), 2738–2749.
- Kwon J., Nayhouse M., Christofides P., and Orkoulas G. (2014). Modeling and control of crystal shape in continuous protein crystallization. *Chemical Engineering Science*, 107, 47-57.
- Liu J., Dai J., Han C., Zhang J. Ai J., Zhai C., Liu X., Sun W. (2020). Simulation of the Crystallization Process based on Cellular Automata --- Snowflake Formation from Pure Water System. *Computer Aided Chemical Engineering*, 48, 187-192.
- Misra S., Zhang D., Qi Z., Li D., Lu J., Chen H., and Wang H. (2020). Morphology Control of Self-Assembled Three-Phase Au-BaTiO<sub>3</sub>-ZnO Hybrid Metamaterial for Tunable Optical Properties. *Crystal Growth & Design*, 20(9): 6101-6108.
- Neumann V.J. (1966) Theory of self-reproducing automata Burks A W (ed.), *University of Illinois Press*.
- Pineau A., Guillemot G., Reinhart G., Regula G., Mangelinck-Noel N., and Gandin Ch.-A. (2020). Three-dimensional cellular automaton modeling of silicon crystallization with grains in twin relationships. *Acta Materialia*, 191, 230-244.
- Rosa C.A., and Braatz R.D. (2018). Multiscale Modeling and Simulation of Macromixing, Micromixing, and Crystal Size Distribution in Radial Mixers/Crystallizers. *Ind. Eng. Chem. Res.*, 57, 5433–5441.
- Tiwary, A.K. and Jindal M. (2012). Crystal Habit Changes and Dosage Form Performance. *Encyclopedia of Pharmaceutical Science and Technology*, 1(4): 1-19.